ORGANOMETALLICS

Article

Cite This: *Organometallics* 2020, 39, 142−152

pubs.acs.org/Organometallics

CH_3−X Reductive Elimination Reactivity of $Pt^{IV}Me$ Complexes Supported by a Sulfonated CNN Pincer Ligand (X = OH, CF_3CO_2, $PhNMe_2^+$)

Jiaheng Ruan, Daoyong Wang, and Andrei N. Vedernikov*

Department of Chemistry and Biochemistry, University of Maryland, College Park, Maryland 20742, United States

Supporting Information

ABSTRACT: Three new dihydrocarbyl $LPt^{IV}Me(Y)$ complexes (**6**−**8**; Y = Cl, I, OCH_2CF_3) supported by the sulfonated CNN pincer ligand L have been prepared and characterized. The reaction of these complexes with a number of nucleophiles (H_2O, $CF_3CO_2^-$, Me_2SO, $PhNMe_2$) resulting in the formation of corresponding C−X coupled products CH_3−X has been studied in 2,2,2-trifluoroethanol (TFE) and DMSO. In TFE or DMSO solutions at 22 °C, in the presence of $PhNMe_2$, a quantitative formation of a C−N coupled product, $PhNMe_3^+$, was observed for **6**−**8**, with the reactivity decreasing in the order **6** > **7** > **8**. The use of NaO_2CCF_3 in TFE solutions was less efficient, leading to the production of MeO_2CCF_3 in 60% yield after 22 h at 70 °C. In DMSO the C−O coupling was high yielding when aqueous trifluoroacetic acid was used to produce methanol (87% after 3 h at 80 °C) or when NaO_2CCF_3 was used to form MeO_2CCF_3 (80% after 1.5 h at 80 °C), with Me_3SO^+ being a minor byproduct. The kinetics study of the reaction between **6**−**8** and $PhNMe_2$ in TFE has revealed an overall second-order rate law, $d[PhNMe_3^+]/dt = k_2[\mathbf{6}, \mathbf{7} \text{ or } \mathbf{8}][PhNMe_2]$, consistent with the realization of an S_N2-type process. A DFT modeling of several alternative pathways of reaction between **7** and $PhNMe_2$ in TFE supported the direct nucleophilic attack of $PhNMe_2$ at the methyl group carbon of **7** as the most likely mechanism of this transformation.

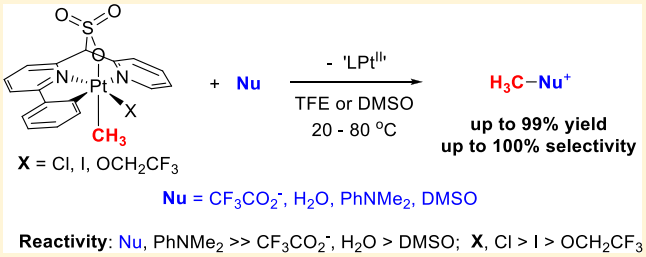

INTRODUCTION

The selective aerobic oxidative CH functionalization of hydrocarbon feedstocks (eq 1) is an important and academically challenging goal.[1]

$$2R{-}H + O_2 + 2HX \rightarrow 2R{-}X + H_2O \quad (1)$$

A Shilov-type Pt-mediated aerobic CH functionalization (Scheme 1) represents a plausible approach to the solution of this problem.[2] Previously, while pursuing the development of Pt-based systems for aerobic oxidative CH functionalization (eq 1), we have designed and prepared the novel Pt(II) aqua complexes **1**−**3** supported by sulfonated CNN pincer ligands (Chart 1) that are ranked as some of the most active catalysts for H/D exchange of various arenes ArH in wet TFE-*d* (TFE = 2,2,2-trifluoroethanol) solutions.[3,4] Importantly, at least in the case of **1**, the derived $[LPt^{II}Ph]^-$ species were shown to react cleanly with O_2 to form a derived Pt(IV) aryl complex, $LPt^{IV}Ph(OH)$. Accordingly, a consecutive arene CH and O_2 activation at a Pt(II) center leading to the isolable Pt(IV) aryl hydroxo complexes $LPt^{IV}Ar(OH)$ (**4**)[5] was demonstrated using complex **1** and a series of arenes (Scheme 2).

Although conceptually important, the system in Scheme 2 has a number of limitations. (a) The TFE derivative of **1**, $LPt^{II}(ROH)$ (R = CH_2CF_3), which is always present in the reaction mixtures, is oxidized concurrently to produce $LPt^{IV}(OR)(OH)$ (**5**), along with **4** (Scheme 2). Complexes **4** and **5** always form in a 1:1 ratio, unless sacrificial reducing agents such as *p*-hydroquinone are present that favor selective

Scheme 1. Catalytic Cycle for Pt-Mediated Oxidative CH Functionalization with O_2

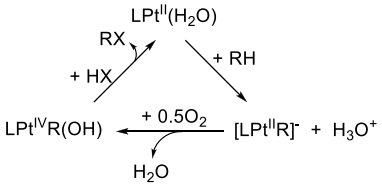

Chart 1. Pt(II) Aqua complexes 1−3 Supported by Sulfonated CNN Pincer Ligands[3,4]

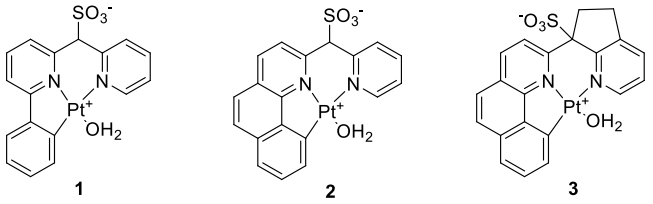

Received: October 18, 2019
Published: December 13, 2019

DOI: 10.1021/acs.organomet.9b00702
Organometallics 2020, 39, 142−152

Scheme 2. Consecutive Arene CH and O_2 Activation at a Pt(II) Center[4]

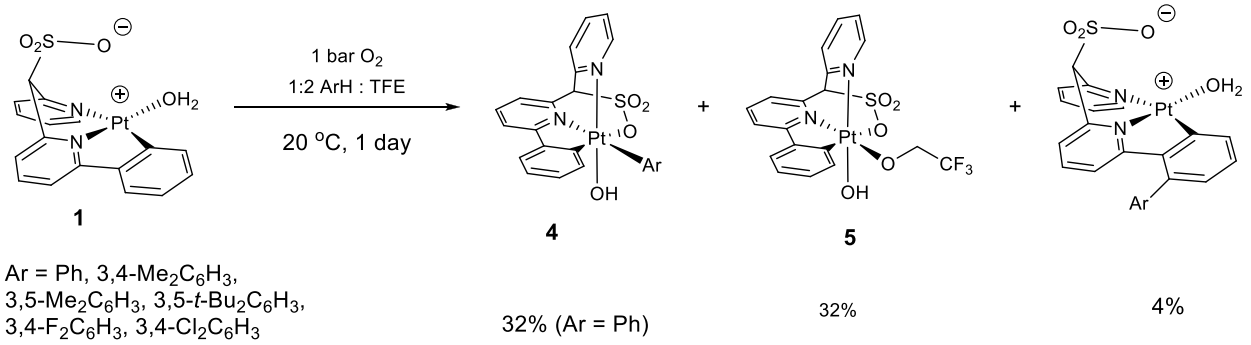

Scheme 3. C−X Reductive Elimination Reactivity of Some $MePt^{IV}$ Complexes

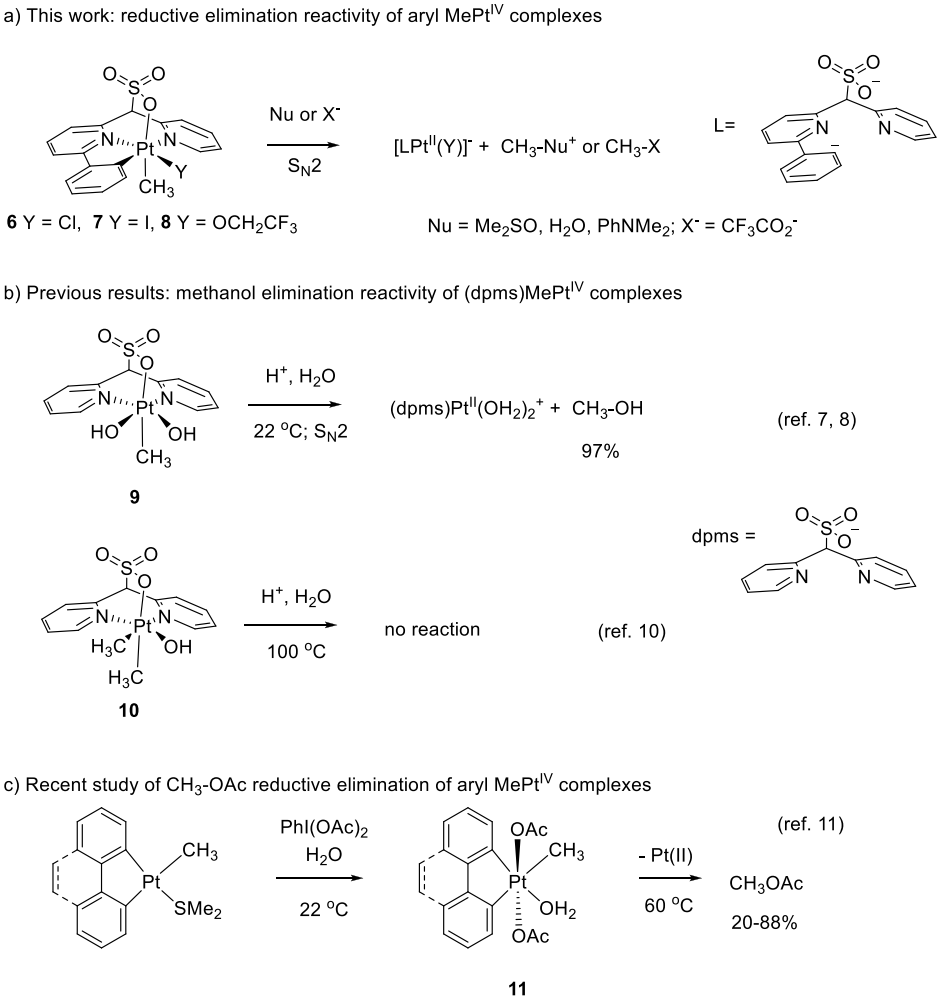

production of **4**. (b) The resulting Pt(IV) aryl hydroxo complexes **4** are inert in C−O reductive elimination.

Among various hydrocarbon substrates that would be interesting to engage in similar stoichiometric (Scheme 2) and, eventually, catalytic (eq 1) transformations, methane is a very attractive target, as it might lead to the development of a better "methane economy".[1,6] To make such chemistry possible, several conditions have to be met. First, engaging methane and the sulfonated CNN Pt(II) pincer aqua complexes in Chart 1 in transformations analogous to the arene chemistry in Scheme 2 should be viable. Next, the derived methane complexes such as $LPt^{IV}Me(Y)$ (**6** (Y = Cl), **7** (Y = I), **8** ($Y = OCH_2CF_3$)) (Scheme 3a) should be able to engage in Me−X coupling, thus avoiding one of the two major problems mentioned above for the arene substrates (Scheme 2). Such Me−X coupling is envisioned to follow an S_N2 mechanism, as reported previously for the analogous complex **9** containing a sulfonated dipyridinemethane ligand, dpms (Scheme 3b),[7,8] and as has been demonstrated by a large body of prior experimental studies involving various $Pt^{IV}Me$ and $Pd^{IV}Me$ complexes.[9]

Considering the feasibility of Me−X coupling of complexes **6**−**8**, one can note, on the one hand, that they have one more hydrocarbyl group at the Pt(IV) center, in comparison to **9**,

DOI: 10.1021/acs.organomet.9b00702
Organometallics 2020, 39, 142−152

Scheme 4. Preparation of Complexes 6−8

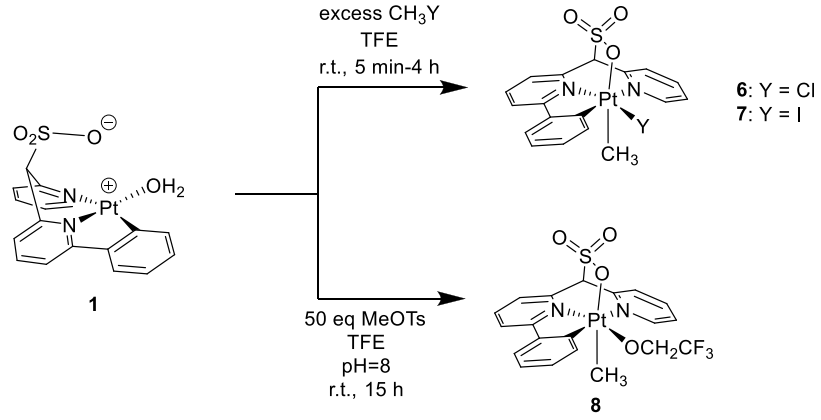

Chart 2. Possible Configurations of $LPt^{IV}Me(Y)$ (6−8)

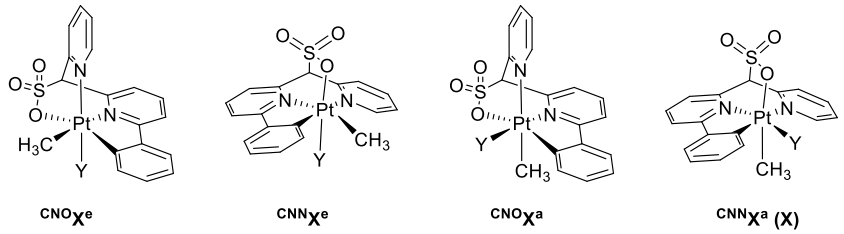

X = **6**, Y = Cl; **X** = **7**, Y = I; **X** = **8**, Y = OCH_2CF_3

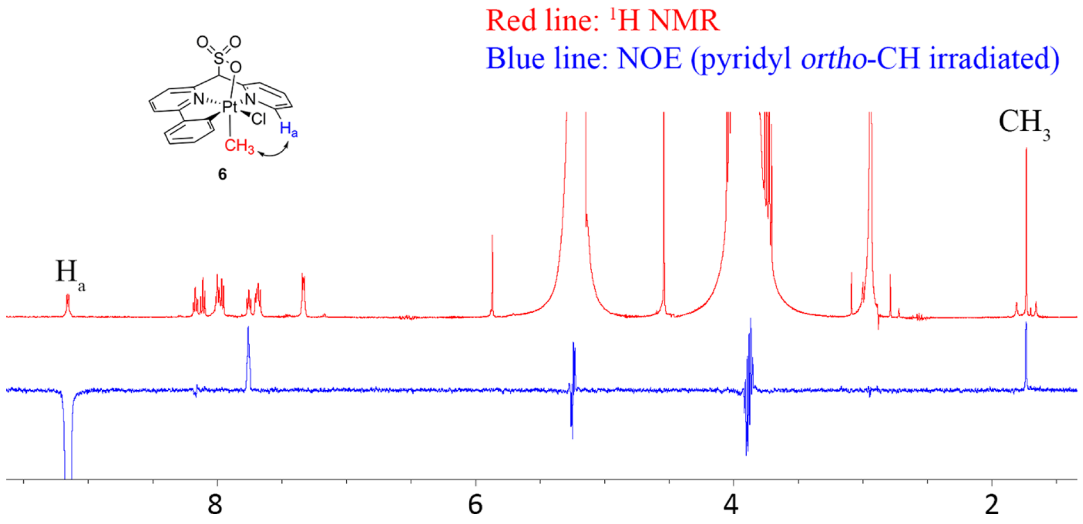

Figure 1. ^{1}H NMR spectrum of **6** (top) and its selective NOE spectrum (bottom).

which makes them more electron rich/less electrophilic and, expectedly, less reactive than **9**. In fact, the presence of two methyl groups at a Pt(IV) center in the dimethyl Pt(IV) complex **10**, an analogue of **9**, renders **10** unreactive toward nucleophilic attacks by water (Scheme 3b).[10]

On the other hand, promisingly, there is a literature report disclosing the CH_3−O reductive elimination of metallacyclic aryl methyl Pt(IV) complexes **11** in benzene and in some weakly to moderately polar solvents, $CHCl_3$, MeCN, and acetone, at 60 °C to produce MeOAc in 20% (acetone)−88% (MeCN) yield (Scheme 3c).[11] In addition, Pt(IV) complexes **4** have been demonstrated to have a pincer-ligand-imposed constrained geometry[3] which is also expected for **6**−**8**. The associated strain should be relieved as a result of the CH_3−X elimination, thus enhancing the reductive elimination reactivity of **6**−**8**. Hence, on the basis of these observations, CH_3−X elimination reactions of complexes **6**−**8**, potentially, may be facile already at room temperature.

To test the hypothesis that complexes **6**−**8** may be involved in CH_3−X coupling under relatively mild conditions, an experimental investigation was needed. To that end, in this work we have prepared the series of model complexes $LPt^{IV}Me(Y)$ (**6**−**8**; Y = Cl, I and OCH_2CF_3), which might result from methane and O_2 activation in the presence of suitable HY, similar to the case in Scheme 1, and explored their reactivity toward various nucleophiles.

DOI: 10.1021/acs.organomet.9b00702
Organometallics 2020, 39, 142−152

Chart 3. $^2J_{195PtH}$ Coupling Constants in $Pt^{IV}Me$ Complexes in Previous Studies[8,10] and This Work

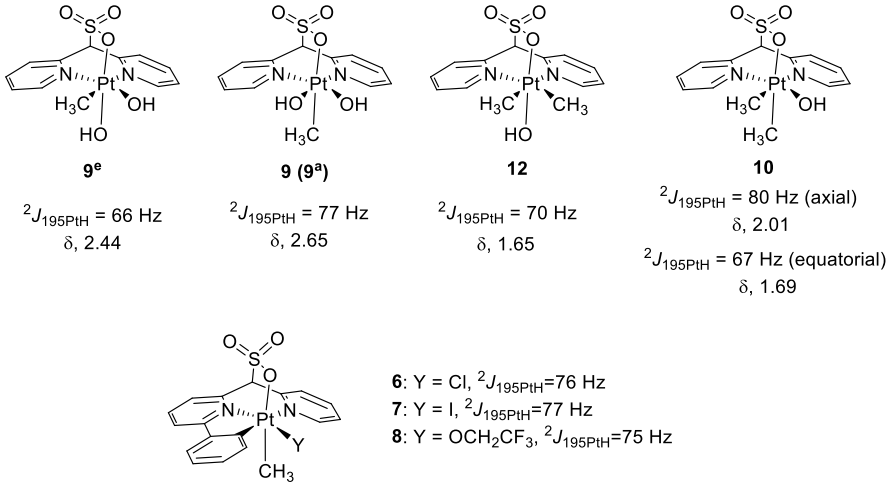

Scheme 5. Generation of Dimethyl Pt(IV) Complexes 14 and 15 from $K[LPt^{II}Me]$, 13, and CH_3I

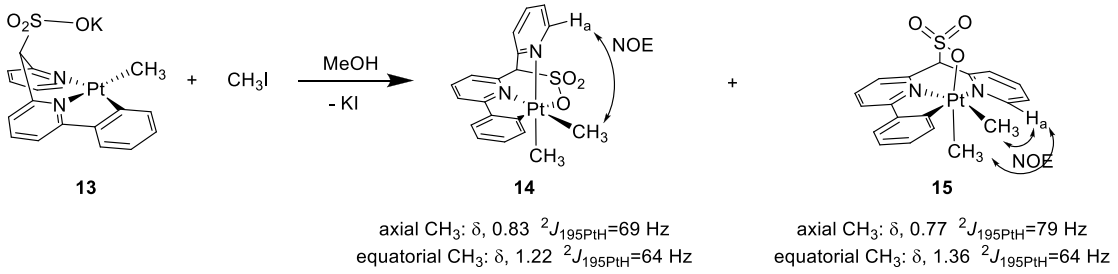

RESULTS AND DISCUSSION

Preparation of 6–8. The preparation of **6** and **7** was carried out by reacting the corresponding methyl halide, CH_3–X, taken in large excess, with $LPt^{II}(H_2O)$ (**1**) dissolved in TFE at 22 °C (Scheme 4). In the course of the reactions the dark red solution of **1** gradually turned yellow to produce **6** or **7**. After all volatiles were removed, **6** and **7** containing TFE molecules of crystallization (see the Experimental Section) were obtained in pure form, according to ^1H NMR, as fine light yellow solids in high isolated yields. **8** was prepared using MeOTs as the methylating reagent. To promote the formation of $LPt^{II}(OCH_2CF_3)^-$, a mixture of **1** and MeOTs in TFE was made weakly basic by the addition of KOH. The reaction was stopped when the conversion reached about 50% to avoid formation of side products. After recrystallization from TFE–diethyl ether, **8** was obtained as a light yellow solid in 22% yield. All three complexes are stable in air as solids but undergo a slow degradation in TFE solutions at 22 °C.

Characterization of 6–8. Our numerous attempts to grow single crystals of complexes **6–8** were not successful (see the Experimental Section). Hence, characterization of the compounds was done using various NMR techniques and mass spectrometry. In terms of the possible configurations of these compounds, four isomeric structures can be envisioned, having either a CNO- or a CNN-coordinated pincer ligand (^{CNO}**X** vs ^{CNN}**X**) and either an equatorial or an axial arrangement of the methyl ligand (**X**^{e} vs **X**^{a}), with respect to the plane defined by three Pt-bound donor atoms of the pincer ligand. The four isomeric structural types considered, ^{CNO}**X**^{e}, ^{CNN}**X**^{e}, ^{CNO}**X**^{a}, and **X** (or ^{CNN}**X**^{a}) (**X** = **6–8**), are shown in Chart 2. On the basis of their NMR characterization described below, the complexes prepared in this work, **6–8**, have been assigned the structural type ^{CNN}**X**^{a}.

First, selective NOE experiments of all three complexes **6–8** showed a positive interaction between the CH_3 ligand and the proton in the ortho position of the pyridyl fragment of the pincer ligand (H_a; see characterization of **6** in Figure 1). This result allowed us to rule out the structural type ^{CNO}**X**^{a}.

Next, the coupling constants between the ^{195}Pt and ^1H nuclei on the CH_3 ligand in complexes **6–8** were analyzed and compared to those in similar dpms-derived Pt(IV) mono- and dimethyl complexes **9**^{a} (**9**), **9**^{e}, **12**, and **10** (Chart 3).[8,10] In these structurally similar complexes the magnitude of the $^2J_{195PtH}$ constants is mostly affected by the nature of the donor atom trans to the CH_3 ligand, as shown below. The Pt(IV) methyl complex **9**^{e} has an equatorial CH_3 ligand with a pyridine nitrogen atom trans to it, whereas its isomer **9**^{a} has an axial CH_3 ligand and an oxygen atom of the sulfonate group trans to it. The analogous isomeric Pt(IV) dimethyl complexes **12** and **10** also have different arrangements of their CH_3 ligands vs pyridine nitrogen and sulfonate oxygen atoms. According to Chart 3, smaller $^2J_{195PtH}$ values of 66–70 Hz are observed in **9**^{e}, **12**, and **10** (the equatorial methyl), in comparison to 77–80 Hz for **9**^{a} and **10** (the axial methyl), which is due to a stronger trans influence of the pyridine nitrogen atom, in comparison to that of the anionic sulfonate oxygen.[8] Notably, the $^2J_{195PtH}$ values found for complexes **6–8** are in the range of 75–77 Hz, similar to those of **9**^{a} and one of the methyls of **10**. This observation points to the most likely arrangement of the CH_3 group trans to the sulfonate oxygen atom in **6–8**. Notably, out of the four structural types shown in Chart 2, only ^{CNN}**X**^{a} has a sulfonate oxygen atom trans to the

DOI: 10.1021/acs.organomet.9b00702
Organometallics 2020, 39, 142–152

Table 1. Reductive Elimination Reactivity of Complexes 6−8

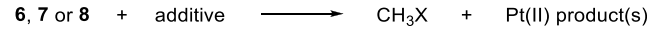

entry	substrate/ concentration, mM	additive	solvent	time, h	T, °C	yield of MeOH/MeOOCCF$_3$/ O=S(CD$_3$)$_2$(CH$_3$)$^+$ at 100% conversion of **6−8**, %
1	**6**/28	0.5 M HBF$_4$, 2.5 M H$_2$O	TFE	9	65	0/−/−[a]
2	**7**/28	0.5 M HBF$_4$, 2.5 M H$_2$O	TFE	32	60	0/−/−[a]
3	**8**/21	0.5 M HBF$_4$, 2.5 M H$_2$O	TFE	6	70	0/−/−[a]
4	**7**/21	0.42 M TFA	TFE	2.5	80	0/0/−[a]
5	**7**/33	0.66 M NaOOCCF$_3$	TFE	22	70	0/60/−
6	**7**/25	0.30 M NaOOCCF$_3$	D$_2$O/AcOH-d_4, 1/2	54	40	0/−/−
7	**6**/12	0.46 M TFA-d	DMSO-d_6	10	80	22/17/0
8	**7**/23	0.46 M TFA	DMSO-d_6	1.5	80	35/34/13
9	**8**/20	0.40 M TFA-d_1	DMSO-d_6	53	80	15/25/5
10	**7**/31	none	DMSO-d_6	3	80	5/0/75
11	**7**/29	0.58 M TFA, 4.6 M H$_2$O	DMSO-d_6	3	80	87/1/10
12	**7**/31	0.62 M NaOOCCF$_3$	DMSO-d_6	1.5	80	15/80/1
13	**6**/4.0	0.26 M PhNMe$_2$	TFE-d	13	22	98[b]
14	**7**/4.6	0.27 M PhNMe$_2$	TFE-d	20	22	99[b]
15	**8**/3.9	0.27 M PhNMe$_2$	TFE-d	29	22	100[b]
16	**7**/13	0.49 M PhNMe$_2$	DMSO-d_6	5	22	98.5[b]

[a]Unidentified precipitate formed. [b]Yield of Me$_3$NPh$^+$.

CH$_3$ ligand. Hence, on the basis of this consideration, complexes **6−8** are, most likely, of the ^{CNN}**X**^{a} type.

To further support the validity of our approach based on the use of $^2J_{195PtH}$ constants for CH$_3$ ligands, in assigning the configuration of complexes in **6−8**, we have also prepared and characterized the derived dimethyl Pt(IV) complexes **14** and **15** (Scheme 5). Similarly to the isomeric complexes in Chart 2, in **14** and **15** their CH$_3$ ligands have either pyridine donors trans to them, two in **14** and one in **15**, or a sulfonate oxygen atom trans to one of the methyls in **15**. These complexes were generated by reacting the methyl Pt(II) precursor K[LPt^{II}Me] (**13**) with CH$_3$I. The methylation reaction was not selective and produced a mixture of **14** and **15** in about a 3:5 ratio. The mixture was characterized by ^{1}H NMR spectroscopy in DMSO-d_6 solutions without separation (Figure S15). The chemical shifts and the Pt−H coupling constants for the protons of methyl ligands of complexes **14** and **15** are given in Scheme 5. Additional 2D NOE experiments (see Figure S16 and S17) of the mixture of **14** and **15** allowed us to assign to complex **14** two weaker CH$_3$ group signals of equal intensity, one at 0.83 ppm and one at 1.22 ppm. In **14**, both CH$_3$ ligands are trans to the pyridyl nitrogen atoms and their $^2J_{195PtH}$ constants, 64 and 69 Hz, are very close to the range of 66−70 Hz observed for **9**^{e} and **12**, also having the CH$_3$ groups trans to the nitrogen atoms, but less than 77−80 Hz for **9**^{a} and **10** (the axial methyl) and 75−77 Hz for **6−8** (Chart 3).

Two remaining and stronger signals of CH$_3$ groups (Figure S15) were assigned to **15**. Notably, the signal at 1.36 ppm has a $^2J_{195PtH}$ value of 64 Hz, close to the range of 66−70 Hz for **9**^{e} and **12**, thus suggesting that this methyl ligand is in an equatorial position, trans to a nitrogen atom. Another signal at 0.77 ppm has a $^2J_{195PtH}$ value of 79 Hz, well in the range of 77−80 Hz observed for the axial methyls in **9**^{a} and **10** having CH$_3$ ligands trans to the sulfonate group.

Overall, this analysis shows that the methyl group $^2J_{195PtH}$ values in Pt(IV) methyl complexes considered can be used consistently to distinguish between the methyl groups positioned trans to pyridine nitrogen and the sulfonate group oxygen atoms in sulfonated pincer complexes above. Altogether, our results point to a conclusion that complexes **6−8** are of the structural type ^{CNN}**X**^{a} (Chart 2).

Reactivity of 6−8 toward O-, S-, and N-Nucleophiles. Unlike LPt^{IV}Ar(OH) (**4**), for which no C−X reductive elimination at the Pt(IV) center was observed, our new Pt(IV) methyl complexes LPt^{IV}Me(Y) (**6−8**) can form C−X coupled products in high yields under mild conditions when they are reacted with suitable nucleophiles in suitable solvents, as described below. The initial choice of solvents for our experiments was dictated by such factors as the solubility of the complexes and the potential of the solvent to also be compatible with other steps of the plausible catalytic cycle in Scheme 1: first of all, the CH activation step. The latter typically requires that the solvent can only weakly coordinate to a Pt(II) center.[12] Some solvents known to be compatible with C−H activation at a Pt(II) center are TFE[3−5] and aqueous acetic and trifluoroacetic (TFA) acids.[12] In terms of the solubility of **6−8**, it is marginal in both TFE and 2/1 acetic acid/water mixtures. In turn, DMSO, although perhaps incompatible with the CH activation chemistry by **6−8**,[3−5] allows for a much better solubility of these complexes and the utilization of ionic nucleophiles such as trifluoroacetate anions. Among the nucleophiles tested in our reactions were water and trifluoroacetate anion, which can be present in aqueous carboxylic acid mixtures, and *N*,*N*-dimethylaniline. The last species was used, among other N-nucleophiles, in our recent tests of electrophilicity of the Shilov reaction intermediate [Pt^{IV}CH$_3$Cl$_5$]$^{2-}$.[13] Notably, DMSO is by itself a nucleophile, and when it was used as a solvent in the absence of strong competitors, nucleophilic reactivity involving DMSO was observed. As we ran our tests, whose results are summarized in Table 1, our goal was to obtain the information about yields attainable after a full conversion of **6−8** and the distribution of

DOI: 10.1021/acs.organomet.9b00702
Organometallics 2020, 39, 142−152

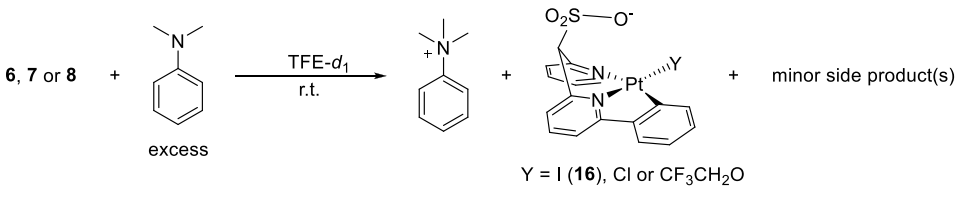

(2)

Scheme 6. Earlier Examples of Me−N Coupling Reactions at d^6 Metal Centers

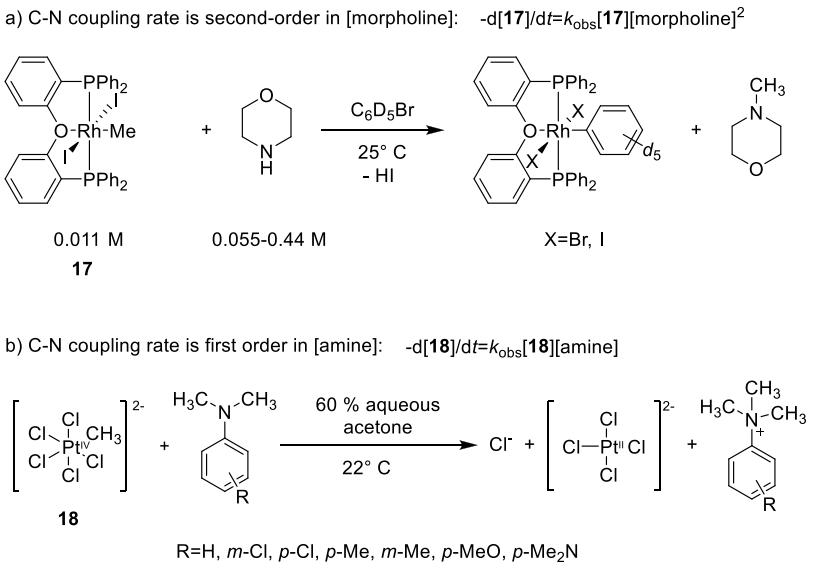

Me−X coupled products. All experiments were performed in Teflon-sealed NMR J. Young tubes. ^{1}H NMR spectroscopy in combination with an internal standard technique was used to monitor the reactions and determine yields of the methylation products CH_3X and conversion of the Pt(IV) methyl complexes.

We first tested the reactivity of **6**−**8** dissolved in TFE toward water as a nucleophile. An additive of 50% aqueous HBF_4 was used to enhance the electrophilicity of these complexes via protonation.[7,8] Unexpectedly, heating the resulting acidic solutions for several hours at 60−70 °C did not yield any CH_3X product. Instead, unidentified TFE-insoluble precipitates formed (Table 1, entries 1−3). The same occurred as the result of using **7** in an attempted reaction with trifluoroacetic acid acting as an electrophilic activator of the $Pt^{IV}Me$ complex and a source of nucleophilic $CF_3CO_2^-$ anions (entry 4). The use of sodium trifluoroacetate as a source of the nucleophile in the absence of other additives was more efficient, with a 60% yield of the ester, MeO_2CCF_3, 8% MeI, and full conversion of **7** at 70 °C (entry 5). The small amounts of MeI could have resulted from a reaction of **7** with iodide anion produced, in turn, in a ligand substitution reaction between excess $CF_3CO_2^-$ anions and $LPt^{II}(I)^-$ (**16**). The latter complex was prepared by us independently and was detected in the reaction mixtures. A few minor products in the reaction of **7** and sodium trifluoroacetate were not identified. The use of aqueous acetic acid (1/2 by volume) as a solvent with sodium trifluoroacetate as a nucleophile did not lead to either MeOH or MeO_2CCF_3 when the full conversion of **7** was achieved at 40 °C (entry 6). Instead, a number of new species formed, including some new unidentified $Pt^{IV}Me$ species in 11% yield. Hence, the weakly nucleophilic trifluoroacetate anion is readily deactivated on going from TFE to a strongly anion stabilizing protic solvent, aqueous AcOH.

Notably, the use of DMSO containing an additive of wet TFA allowed us to retain all Pt species in solution and accomplish an efficient electrophilic activation by TFA of all three $Pt^{IV}Me$ complexes **6**−**8** toward their nucleophilic attacks by water, $CF_3CO_2^-$, and DMSO (Table 1, entries 7−9). The formation of the corresponding CH_3−X coupling products was observed: MeOH in 15−35% yield, MeO_2CCF_3 in 17−34% yield, and Me_3SO^+ in up to 13% yield after the full conversion at 80 °C. Notably, in the absence of TFA, complex **7** produced mostly Me_3SO^+, which formed in 75% yield (entry 10). In turn, when the concentration of water was raised to 4.6 M (10 vol %) in TFA-containing mixtures, the reaction of **7** was directed toward the selective formation of MeOH (87%, entry 11). Finally, combining **7** with NaO_2CCF_3 as a nucleophile in DMSO solution in the absence of other additives allowed us to increase the yield of MeO_2CCF_3 up to 80% (entry 12). On the basis of the product distribution given in entries 11 and 12, the observed nucleophilicity trend is H_2O, $CF_3CO_2^-$ > DMSO with the nucleophilicity of $CF_3CO_2^-$ strongly diminished in the presence of water additives.

Since none of the reactions above could afford Me−X products in yields higher than 80−87%, we decided to use a stronger nucleophile, *N*,*N*-dimethylaniline, with an expectation of observing faster and cleaner C−X elimination reactions. Indeed, in the presence of 0.3 M *N*,*N*-dimethylaniline all of the complexes **6**−**8** used as 4−5 mM solutions in TFE reacted to produce the derived *N*,*N*,*N*-trimethylanilinium salts (eq 2) in a virtually quantitative yield (NMR) at 22 °C (Table 1, entries 13−15). In DMSO solution the reaction of the aniline with **7** was also efficient (entry 16), with the major Pt(II)-containing product being $LPt^{II}(I)^-$ (**16**).

DOI: 10.1021/acs.organomet.9b00702
Organometallics 2020, 39, 142−152

Hence, the performed experiments have demonstrated the ability of aryl methyl Pt(IV) complexes **6**–**8** to undergo C–O coupling with water and trifluoroacetate anion to produce methanol and methyl trifluoroacetate, respectively, in DMSO solutions at 80 °C. A fast and clean formation of products with new Me–N bonds (eq 2) was also observed already at 22 °C when *N,N*-dimethylaniline was used as a nucleophile in either DMSO or TFE solutions.

Having demonstrated a clean Me–N coupling of complexes **6**–**8** and $PhNMe_2$ under mild conditions, we next turned our attention to the reaction kinetics analysis. Previously, reactivity studies of the $Rh^{III}Me(I)_2$ complex **17** have shown an overall third-order kinetics of its reaction with secondary amines (Scheme 6, a).[14] In turn, our own study of the reaction of $PtMeCl_5^{2-}$ (**18**) and various N-nucleophiles (Scheme 6b) has shown first-order reaction kinetics with respect to both [**18**] and substituted anilines.[13] It was of our interest to determine what would be the rate law for the reaction in eq 2.

In our kinetics experiments we used TFE-*d* as a solvent. The disappearance of complexes **6**–**8** in their reaction with a large excess of $PhNMe_2$ was monitored by ^1H NMR spectroscopy for 2–3 reaction half-lives; *tert*-butylbenzene was used as an internal standard (Figure 2). Pseudo-first-order reaction kinetics was observed for all three complexes, as illustrated in Figure 2a–c. For complex **7** the observed pseudo-first-order reaction rate constants were shown to be proportional to [$PhNMe_2$] (Figure 2d), thus implying an overall second-order rate law for the reaction of **7** and $PhNMe_2$, as expected for an S_N2 mechanism. The same overall rate law and the mechanism are proposed in this work for complexes **6** and **8**. The corresponding second-order rate constants for reactions of **6**–**8** with $PhNMe_2$ are given in Table 2. The observed reactivity order, **6** > **7** > **8**, matches the decreasing electron-withdrawing power of the ancillary ligands, Cl > I > OCH_2CF_3.

DFT Analysis of the Reaction Mechanism. The C–N bond formation resulting from the reaction of the representative complex **7** and $PhNMe_2$ was explored by us computationally (DFT). Several potential C–N coupling reaction pathways as well as a C–C coupling of **7** have been analyzed and are illustrated in Scheme 7.

The direct S_N2-type nucleophilic attack of $PhNMe_2$ at the methyl carbon of the complex **7** (path *a*) leading to an ion pair, [$PhNMe_3^+$,$LPt^{II}(I)^-$], has a calculated Gibbs activation energy of 21.4 kcal/mol, very close to the experimentally observed value of 22.0 kcal/mol (Table 2). Hence, this path may correspond to the most likely reaction mechanism. An alternative pathway including a prior isomerization of **7** to $^{CNO}\mathbf{7}^{a}$, with a subsequent nucleophilic attack of $PhNMe_2$ at the methyl carbon of the latter (path *b*), has an overall higher activation energy, 26.9 kcal/mol, thus making this path less probable. Notably, the isomeric $^{CNO}\mathbf{7}^{a}$ can be involved in a C–C coupling reaction leading to the loss of the methyl ligand (path *c*). The reaction intermediate **19** is expected then to undergo a cycloplatination and produce a methylated analogue of **16**. The calculated overall reaction activation energy for path *c* is 24.1 kcal/mol, which makes it less competitive than path *a*, consistent with the absence of C–C coupling products and a 100% reaction selectivity for the observed C–N coupling.

Using an analogy with the reaction between $LRh^{III}Me(I)_2$ complex **17** and secondary amines (Scheme 6a)[14] that was proposed to involve Rh(III) ammine intermediates and has an overall second reaction order in [amine], we considered path *d* leading from **7** to the ammine adduct **20** (ΔG = 6.8 kcal/mol).

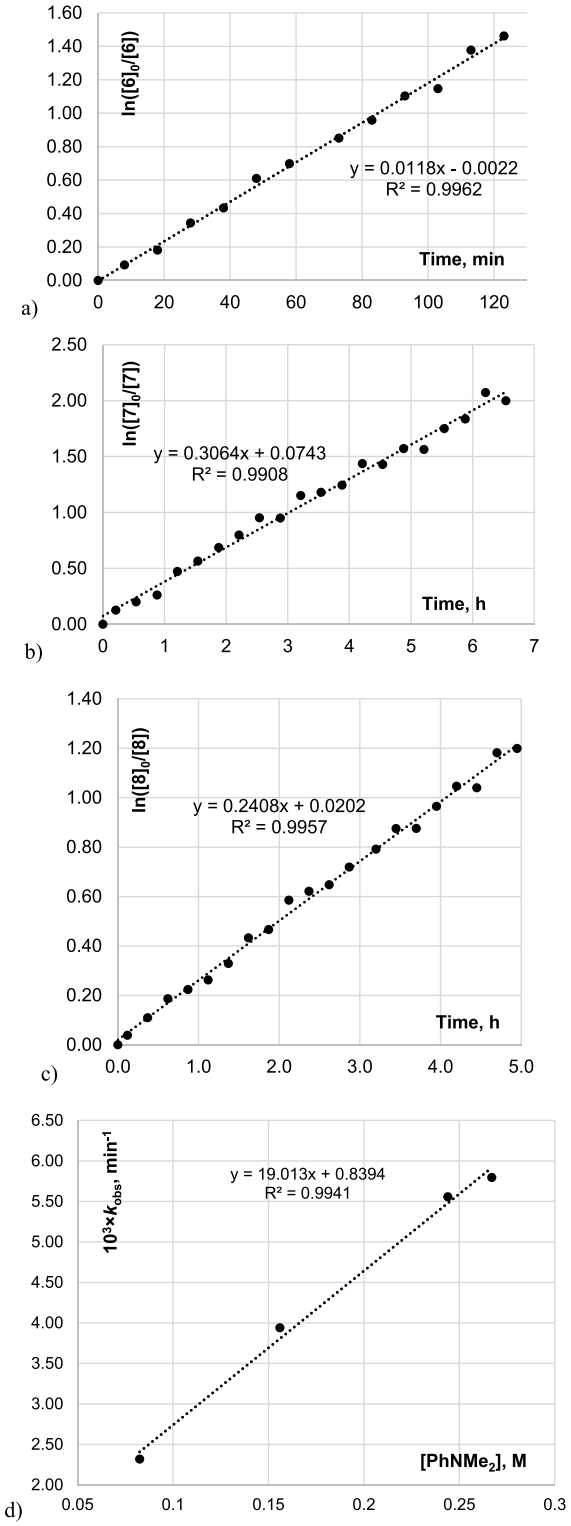

Figure 2. Kinetic plots of reactions between **6**–**8** and *N,N*-dimethylaniline in TFE-*d* (eq 2): (a) 0.048 M **6** and 4.7 M (98 equiv) *N,N*-dimethylaniline; (b) 0.046 M **7** and 2.7 M (58 equiv) *N,N*-dimethylaniline; (c) 0.014 M **8** and 0.67 M (48 equiv) *N,N*-dimethylaniline; (d) plot of k_{obs} for the reaction of **7** with $PhNMe_2$ vs [$PhNMe_2$].

The intermediate **20** then can be involved in an S_N2 attack by a second equivalent of $PhNMe_2$. The calculated Gibbs activation energy for path *d* is 26.8 kcal/mol, which is noticeably higher

DOI: 10.1021/acs.organomet.9b00702
Organometallics 2020, 39, 142–152

Table 2. Second-Order Rate Constants k_2 for the Pt^{IV} to N Methyl Transfer Involving Complexes 6−8 and *N,N*-Dimethylaniline (Eq 2) in TFE-*d* at 22 °C

	6	7	8
second-order rate constant k_2 (M^{-1} min^{-1})	0.0274 ± 0.0005	0.0189 ± 0.0009	0.0046 ± 0.0001
$\Delta G^{\ddagger}_{298}$, kcal/mol	21.8	22.0	22.8

Scheme 7. Potential Reaction Pathways of Complex 7 Leading to C−N and C−C Coupling[a]

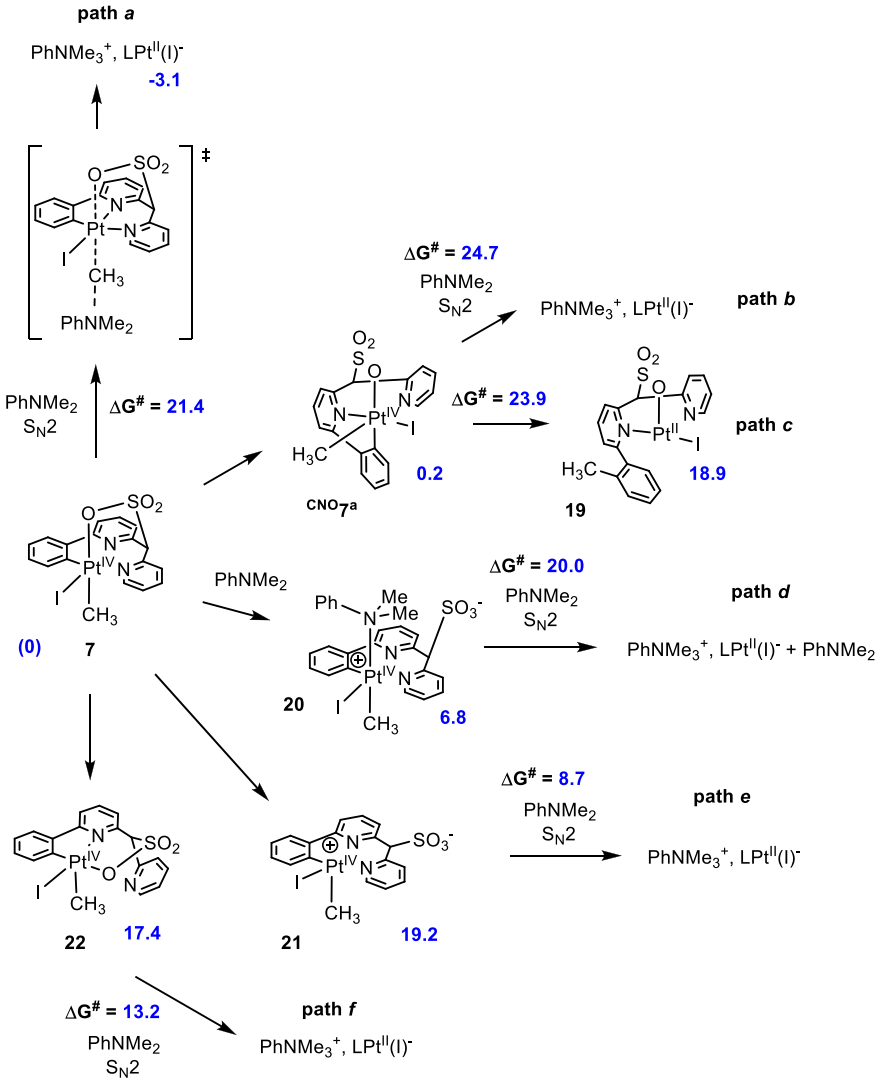

[a]The standard reaction Gibbs energies (blue font) are for TFE solutions, in kcal/mol.

than that for path *a*. Hence, path *d* can also be ruled out for eq 2.

The reaction of **7** with $PhNMe_2$ might also involve five-coordinate $Pt^{IV}Me$ transients, either a CNN-coordinated **21** (path *e*) or a CNO-coordinated **22** (path *f*). In the case of path *e* the respective five-coordinate intermediate **21** is 19.2 kcal/mol higher in energy than **7**, which is the energy penalty for the broken Pt^{IV}−O bond not counteracted by any possible entropy gain at this step because of the chelate structure of **7**. The following step involving five-coordinate intermediate **21** and $PhNMe_2$ has a Gibbs activation energy of only 8.7 kcal/mol, but the overall activation energy for path *e*, including the S_N2 step, is 27.9 kcal/mol. Hence, this path also appears to be out of competition with path *a*. The same applies to path *f* with a Gibbs energy for the intermediate **22** of 17.4 kcal/mol and an overall activation barrier for this path of 30.6 kcal/mol.

In summary, we can conclude, on the basis of the results of our DFT calculations, as well as our kinetics study, that a direct S_N2 attack of the aniline at the methyl carbon of complex **7** (path *a*) is the most likely reaction pathway realized in TFE solutions of **7**.

CONCLUSIONS

In summary, in this work we have been able to confirm that the presence of the sulfonated CNN pincer ligand L at a Pt(IV) center renders the derived dihydrocarbyl $LPt^{IV}(CH_3)(Y)$ complexes (Y = Cl, I, OCH_2CF_3) sufficiently reactive toward such nucleophiles as water and $CF_3CO_2^-$ anion in TFE and/or DMSO solutions, thus allowing to produce methanol of methyl

DOI: 10.1021/acs.organomet.9b00702
Organometallics 2020, 39, 142−152

trifluoroacetate as the C−O coupled reaction products in high although not quantitative yields. In turn, a much stronger nucleophile, $PhNMe_2$, reacts with these complexes at a much faster rate, under milder conditions to produce $PhNMe_3^+$ in a virtually quantitative yield. The observed reactivity series **6** (Y = Cl) > **7** (Y = I), **8** (Y = OCH_2CF_3) is expected for an S_N2 reaction mechanism, which also our kinetics study and DFT modeling of the reaction between **7** and $PhNMe_2$ point out. These results are encouraging some further development of the sulfonated CNN pincer ligand platform to enable also a methane CH activation which, so far, was not observable with the current pincer ligand Pt(II) derivatives. Our work targeting this goal is ongoing.

EXPERIMENTAL SECTION

General Considerations. Reactions requiring exclusion of air and/or moisture were carried out under an argon atmosphere. All reagents for which synthesis is not reported were purchased from Sigma-Aldrich, Oakwood Chemical, Matrix Scientific, or Pressure Chemical and used without purification unless otherwise noted. Silica gel SEPIX 56040 (63 μm) was purchased from ZEOCHEM and used for all column chromatography purifications. TFE from Sigma-Aldrich or Oakwood Chemical was dried over calcium hydride, purified by vacuum transfer, and stored in an argon-filled glovebox. THF solvent was dried over and distilled from sodium/benzophenone adduct and stored over molecular sieves under argon. The deuterium-labeled solvents MeOD-d_4, $CDCl_3$, and DMSO-d_6 were purchased from Cambridge Isotope Laboratories, and CF_3CH_2OD (TFE-*d*) was purchased from Sigma-Aldrich. ^{1}H NMR (400, 500, and 600 MHz), ^{13}C NMR (100, 125, and 150 MHz), and ^{19}F NMR (376 MHz) spectra were recorded on a Bruker AVANCE 400 MHz, a Bruker DRX-500 MHz, or a Bruker AVIII-600 MHz spectrometer. Chemical shifts are reported in parts per million (ppm) (δ) and referenced to residual solvent peaks. Multiplicities are reported as follows: br (broad signal), s (singlet), d (doublet), t (triplet), q (quartet), quin (quintet), sex (sextet), m (multiplet), dd (doublet of doublets), dt (doublet of triplets), qd (quartet of doublets). Coupling constants (J) are reported in Hz. High-resolution mass spectrometry (HRMS) experiments were performed using a JEOL AccuTOF-CS instrument.

(C_6H_4-dpms)$Pt^{II}(H_2O)$ (1). The synthesis of this complex was performed according to the literature.[3]

(C_6H_4-dpms)Pt^{IV}(Me)Cl (6). In a glovebox, 5 mg (9.3 μmol) of complex **1** was placed in a vial and dissolved in 0.7 mL of TFE to form a dark orange solution. The solution was transferred into an NMR J. Young tube and then removed from the glovebox. CH_3Cl was bubbled into the solution for about 10 min until the solution turned red. The NMR J. Young tube was Teflon capped. As the reaction progressed, the solution turned yellow. The transformation was quantitative by ^{1}H NMR after 4 h. Yield of **6**·0.70TFE: 5.0 mg (8.8 μmol, 95%). Our attempts at growing single crystals of **6** from TFE solutions using vapor diffusion (Et_2O) were not successful. The composition of **6**·0.70TFE was estimated using ^{1}H NMR integration of a solution prepared by dissolution in DMSO-d_6 a preweighed sample of the complex and *tert*-butylbenzene used as an internal standard. ^{1}H NMR (500 MHz, 22 °C, CF_3CH_2OD): δ 9.15 (d, $^3J_{HH}$ = 5.6 Hz, 1H, pyridyl-*ortho* H), 8.17 (dt, J_{HH} = 7.7 Hz, J_{HH} = 1.4 Hz, 1H, ArH), 8.11 (t, J_{HH} = 7.8 Hz, 1H, ArH), 8.05−7.93 (m, 3H, ArH), 7.75 (dt, J_{HH} = 6.5 Hz, J_{HH} = 0.9 Hz, 1H, ArH), 7.72−7.64 (m, 2H, ArH), 5.86 (s, 1H, $CHSO_3$), 1.73 (s, $^2J_{195PtH}$ = 76 Hz, 3H, $PtCH_3$). ^{13}C NMR (150 MHz, 22 °C, CF_3CH_2OD): δ 168.0, 150.7, 150.3, 144.7, 144.6, 143.4, 141.2, 134.2, 133.4, 129.4, 127.6, 122.4, 75.7, 6.0 (with satellites, J_{PtC} = 570 Hz). ESI-MS of **6** in TFE solution with $NaBF_4$ added: $[6 + Na]^+$, 593.0050; calculated for $[6 + Na]^+$, $C_{18}H_{16}ClN_2NaO_3PtS$, 593.0030.

(C_6H_4-dpms)Pt^{IV}(Me)I (7). In a glovebox, 50 mg (93.2 μmol) of complex **1** was placed in a vial and dissolved in 5 mL of TFE to form a dark orange solution. A 20 μL portion (0.32 mmol, 3.4 equiv) of CH_3I was added to the solution. The solution turned red and then yellow in less than 1 min. Volatiles were removed under vacuum, and the product appeared as a light yellow solid, **7**·0.35TFE. Yield: 60 mg (90.7 μmol, 97%). Our attempts at growing single crystals of **7** from TFE solutions using slow evaporation, solvent or vapor diffusion (Et_2O), and reactant (MeI) diffusion into a TFE solution of **1** were not successful. The 98% purity of **7**·0.35TFE was estimated using ^{1}H NMR integration of a solution prepared by dissolution in DMSO-d_6 a preweighed sample of the complex and *tert*-butylbenzene used as an internal standard. ^{1}H NMR (400 MHz, 22 °C, DMSO-d_6): δ 9.42 (d, $^3J_{HH}$ = 5.4 Hz, 1H, pyridyl-*ortho* H), 8.59 (d, 7.9 Hz, $^3J_{195PtH}$ = 37 Hz, 1H, ArH), 8.43−8.35 (m, 3H, ArH), 8.14 (d, J_{HH} = 7.6 Hz, 1H, ArH), 8.01 (d, J_{HH} = 7.7 Hz, 1H, ArH), 7.93−7.82 (m, 2H, ArH), 7.34 (t, J_{HH} = 7.3 Hz, 1H, ArH), 7.26 (dt, J_{HH} = 0.8 Hz, J_{HH} = 7.4 Hz, 1H, ArH), 6.62 (s, 1H, $CHSO_3$), 1.68 (s, $^2J_{195PtH}$ = 76 Hz, 3H, $PtCH_3$). ^{1}H NMR (500 MHz, 22 °C, CF_3CH_2OD): δ 9.57 (d, $^3J_{HH}$ = 5.7 Hz, 1H, pyridyl-*ortho* H), 8.76 (d, J = 8.0 Hz, $^3J_{195PtH}$ = 38 Hz, 1H, ArH), 8.20−8.10 (m, 2H, ArH), 7.98 (d, J_{HH} = 7.8 Hz, 1H, ArH), 7.93 (d, J_{HH} = 8.0 Hz, 1H, ArH), 7.73−7.61 (m, 3H, ArH), 7.28 (t, J_{HH} = 7.6 Hz, 1H, ArH), 7.20 (t, J_{HH} = 7.3 Hz, 1H, ArH), 5.86 (s, 1H, $CHSO_3$), 1.88 (s, $^2J_{195PtH}$ = 77 Hz, 3H, $PtCH_3$). ^{13}C NMR (100 MHz, 22 °C, CF_3CH_2OD): δ 167.2, 154.8, 150.7, 149.2, 144.9, 144.4, 143.4, 141.0, 139.5, 134.1, 129.6, 128.7, 127.9, 127.5, 126.0, 122.6, 75.5, 1.2. ESI-MS of **7** in TFE with HBF_4 added: $[7 + H]^+$, 661.9604; calculated for $[7 + H]^+$, $C_{18}H_{16}IN_2O_3PtS$, 661.9574.

(C_6H_4-dpms)Pt^{IV}(Me)(OCH_2CF_3) (8). In a glovebox, 100 mg (0.186 mmol) of **1** was placed in a vial and dissolved in 2.5 mL of TFE to form a dark orange solution. A 1.71 g portion (9.2 mmol, 50 equiv) of methyl *p*-toluenesulfonate was added to the solution to generate a red color. KOH dissolved in TFE was added to the solution to adjust the pH to 8. The solution turned orange. In about 15 h, the solution was concentrated to ∼1.5 mL and 5 mL of diethyl ether was added to precipitate out the product. The mixture was separated by vacuum filtration, and the solid was washed first two times with diethyl ether and then with a few drops of water. The product was dissolved in TFE and crystallized by slow vapor diffusion of Et_2O. The solid was separated and vacuum-dried at room temperature. Yield: 25 mg (39 μmol), 21%. Our attempts at growing single crystals of **8** from TFE solutions using slow evaporation and vapor diffusion (Et_2O) were not successful. The 99% purity of **8** was estimated using ^{1}H NMR integration of a solution prepared by dissolution in DMSO-d_6 a preweighed sample of the complex and *tert*-butylbenzene used as an internal standard. ^{1}H NMR (400 MHz, 22 °C, TFE-*d*): δ 8.93 (d, $^3J_{HH}$ = 5.5 Hz, 1H, pyridyl-*ortho* H), 8.20 (t, $^3J_{HH}$ = 7.9 Hz, 1H, ArH), 8.08 (t, $^3J_{HH}$ = 8.0 Hz, 1H, ArH), 7.97 (m, 2H, ArH), 7.83 (t, $^3J_{HH}$ = 6.4 Hz, 1H, ArH), 7.73 (d, $^3J_{HH}$ = 7.5 Hz, 1H, ArH), 7.65 (m, 2H, ArH), 7.42 (t, $^3J_{HH}$ = 7.3 Hz, 1H, ArH), 7.37 (t, $^3J_{HH}$ = 7.4 Hz, 1H, ArH), 5.85 (s, 1H, $CHSO_3$), 1.59 (s, $^2J_{195PtH}$ = 75 Hz, 3H, $PtCH_3$). ^{1}H NMR (500 MHz, 22 °C, DMSO-d_6): δ 8.86 (d, $^3J_{HH}$ = 4.6 Hz, 1H, pyridyl-*ortho* H), 8.43−8.26 (m, 3H, ArH), 8.16 (d, J = 7.6 Hz, 1H, ArH), 8.04−7.95 (m, 2H, ArH), 7.89 (dd, J_{HH} = 7.3 Hz, J_{HH} = 1.2 Hz, 1H, ArH), 7.58 (d, J_{HH} = 7.6 Hz, 1H, ArH), 7.43 (t, J_{HH} = 7.3 Hz, 1H, ArH), 7.37 (t, J_{HH} = 7.4 Hz, 1H, ArH), 6.57 (s, 1H, $CHSO_3$), 4.07 (m, 1H, OCH_2CF_3), 3.90 (m, 1H, OCH_2CF_3), 1.29 (s, $^2J_{195PtH}$ = 74 Hz, 3H, $PtCH_3$). ^{13}C NMR (100 MHz, 22 °C, CF_3CH_2OD): δ 168.5, 151.5, 150.8, 148.6, 144.5, 144.4, 143.5, 141.5, 133.4, 132.0, 129.4, 128.5, 128.4, 127.6, 126.5, 122.1, 75.7, 7.6. ^{19}F NMR (100 MHz, 22 °C, CF_3CH_2OD): δ 75.1 (t, $^3J_{FH}$ = 8.3 Hz, OCH_2CF_3). ESI-MS of **8** in TFE solution with $NaBF_4$ added: $[8 + Na]^+$, 656.0406; calculated for $[8 + Na]^+$, $C_{20}H_{17}F_3N_2O_4PtSNa$, 656.0407.

K[(C_6H_4-dpms)Pt^{II}Me] (13). The preligand H_2L[3] and $Pt_2Me_4(SMe_2)_2$[15,16] were synthesized according to the literature. In a glovebox, the preligand H_2L (0.490 g, 1.50 mmol), KO*t*Bu (0.168 g, 1.50 mmol), and a stir bar were placed in a vial. $Pt_2Me_4(SMe_2)_2$ (287 mg, 0.50 mmol) was placed in a separate vial in the glovebox. MeOH was placed in two vials. The suspension of $Pt_2Me_4(SMe_2)_2$ was transferred to the other vial and a total volume of 8 mL of MeOH was used. The mixture was capped and stirred for 5 days. A yellow suspension formed, and the solution was filtered. The filter cake was collected, dried under vacuum at room temperature, and appeared as

DOI: 10.1021/acs.organomet.9b00702
Organometallics 2020, 39, 142−152

a yellow solid. Yield: 350 mg (0.61 mmol), 61%. ^{1}H NMR (600 MHz, 22 °C, MeOD-d_4): δ 9.03 (d, $^3J_{HH}$ = 5.7 Hz, 1H, pyridyl-*ortho* H), 8.04 (dt, J_{HH} = 1.7 Hz, $^3J_{HH}$ = 7.6 Hz, 1H, ArH), 7.96 (t, $^3J_{HH}$ = 7.9 Hz, 1H, ArH), 7.88 (dd, $^3J_{HH}$ = 8.2 Hz, J_{HH} = 0.9 Hz, 1H, ArH), 7.85 (dd, $^3J_{HH}$ = 8.0 Hz, J_{HH} = 0.8 Hz, 1H, ArH), 7.73 (dd, $^3J_{HH}$ = 7.6 Hz, J_{HH} = 0.9 Hz, J_{195PtH} = 59 Hz, 1H, ArH), 7.64 (dd, $^3J_{HH}$ = 7.9 Hz, J_{HH} = 1.2 Hz, 1H, ArH), 7.60 (dd, $^3J_{HH}$ = 7.6 Hz, J_{HH} = 0.9 Hz, 1H, ArH), 7.44 (m, 1H, ArH), 7.09 (dt, $^3J_{HH}$ = 7.4 Hz, J_{HH} = 1.3 Hz, 1H, ArH), 7.01 (dt, $^3J_{HH}$ = 7.5 Hz, J_{HH} = 0.7 Hz, 1H, ArH), 5.88 (s, 1H, $CHSO_3$), 1.13 (s, $^2J_{195PtH}$ = 80 Hz, 3H, $PtCH_3$). ^{13}C NMR (150 MHz, 22 °C, MeOD-d_4): δ 166.3, 154.2, 151.4, 150.9, 148.2, 145.7, 138.5, 138.4, 134.7, 131.1, 126.8, 125.8, 124.9, 123.5, 118.6, 78.9, −8.4. ESI-MS of **13** in MeOH solution: $[(C_6H_4\text{-dpms})Pt^{II}Me]^-$, 534.0465; calculated for $[(C_6H_4\text{-dpms})Pt^{II}Me]^-$, $C_{18}H_{15}N_2O_3PtS$, 534.0451.

Reaction of K[(C_6H_4-dpms)Pt^{II}Me] (13) with CH_3I: Formation of 14 and 15. A 5.0 mg portion (8.7 mmol) of **13** was mixed with 2.0 mL of MeOH. A 0.011 mL portion of CH_3I (0.18 mmol, 20 equiv) was added to the suspension with stirring. The solid fully dissolved after addition of CH_3I and the solution turned from yellow to colorless. The product appeared as a white precipitate 2 min later. It was collected by filtration, washed with methanol, and dried under vacuum. The resulting mixture consists of two products, **14** and **15**, in about a 3:5 ratio. Yield: 3.2 mg, 66%. The following is a partial assignment of ^{1}H NMR signals. Data for **14** are as follows. ^{1}H NMR (400 MHz, 22 °C, DMSO-d_6): δ 8.79 (d, $^3J_{HH}$ = 5.2 Hz, 1H, pyridyl-*ortho* H), 8.16 (dt, $^3J_{HH}$ = 6.0 Hz, $^4J_{HH}$ = 1.7 Hz, 1H, ArH), 8.00 (m, 1H, ArH), 7.89 (d, $^3J_{HH}$ = 7.2 Hz, 1H, ArH), 7.86 (m, 1H, ArH), 7.60 (t, $^3J_{HH}$ = 4.4 Hz, 1H, ArH), 7.47 (d, $^3J_{HH}$ = 7.7 Hz, 1H, ArH), 7.44 (d, $^3J_{HH}$ = 7.4 Hz, 1H, ArH), 7.26 (m, 1H, ArH), 7.19 (t, $^3J_{HH}$ = 7.2 Hz, 1H, ArH), 6.66 (s, $CHSO_3$), 1.22 (s, $^2J_{195PtH}$ = 64 Hz, $PtCH_3$), 0.83 (s, $^2J_{195PtH}$ = 69 Hz, $PtCH_3$). Data for **15** are as follows. ^{1}H NMR (400 MHz, 22 °C, DMSO-d_6): δ 8.76 (d, $^3J_{HH}$ = 5.9 Hz, 1H, pyridyl-*ortho* H), 8.32 (m, 2H, ArH), 8.25 (t, $^3J_{HH}$ = 7.7 Hz, 1H, ArH), 8.21 (m, 1H, ArH), 8.13 (d, $^3J_{HH}$ = 5.2 Hz, 1H, ArH), 7.99 (m, 1H, ArH), 7.85 (m, 1H, ArH), 7.82 (t, $^3J_{HH}$ = 6.4 Hz, 1H, ArH), 7.30 (dt, $^3J_{HH}$ = 5.0 Hz, $^4J_{HH}$ = 1.4 Hz, 1H, ArH), 7.26 (m, 1H, ArH), 6.39 (s, $CHSO_3$), 1.36 (s, $^2J_{195PtH}$ = 64 Hz, $PtCH_3$), 0.77 (s, $^2J_{195PtH}$ = 79 Hz, $PtCH_3$).

K[(C_6H_4-dpms)Pt^{II}(I)] (16). In a 50 mL round-bottom flask were placed 1 equiv of K[$(C_6H_4$-dpms)Pt^{II}(Cl)][3] (25 mg, 0.042 mmol), 5 equiv of KI (34.9 mg, 0.210 mmol), 5 mL of H_2O, and 0.5 mL of TFE. The mixture was heated at 50 °C for 4 h. A PTFE syringe filter was used to filter off the liquid. The solid was dissolved in TFE, and the solution was layered with Et_2O. Crystals formed slowly and then were collected by filtration. Yield: 15 mg (0.022 mmol), 52%. ^{1}H NMR (400 MHz, 22 °C, TFE-*d*): δ 9.95 (d, $^3J_{HH}$ = 5.5 Hz, 1H, pyridyl-*ortho* H), 8.64 (d, $^3J_{HH}$ = 7.8 Hz, 1H, ArH), 7.97 (q, $^3J_{HH}$ = 7.6 Hz, 2H, ArH), 7.74 (t, $^3J_{HH}$ = 7.5 Hz, 2H, ArH), 7.48 (t, $^3J_{HH}$ = 8.3 Hz, 2H, ArH), 7.36 (t, $^3J_{HH}$ = 7.1 Hz, 1H, ArH), 7.10 (t, $^3J_{HH}$ = 7.4 Hz, 1H, ArH), 7.02 (t, $^3J_{HH}$ = 7.6 Hz, 1H, ArH), 5.70 (s, 1H, $CHSO_3$). ^{13}C NMR (100 MHz, 22 °C, CF_3CH_2OD): δ 168.6, 157.5, 151.5, 149.8, 147.2, 142.9, 140.6, 140.4, 138.2, 131.7, 130.4, 126.7, 125.8, 125.6, 120.0, 78.7. ESI-MS of **16** in TFE solution: $[(C_6H_4\text{-dpms})Pt^{II}I]^-$, 645.9267; calculated for $[(C_6H_4\text{-dpms})Pt^{II}I]^-$, $C_{17}H_{12}IN_2O_3PtS$, 645.9263.

Reaction of (C_6H_4-dpms)Pt^{IV}(Me)X (6−8; X = Cl, I, OCH_2CF_3) with Nucleophiles. *General Procedure.* $(C_6H_4$-dpms)Pt^{IV}MeX (**6**−**8**; X = Cl, I, OCH_2CF_3) was combined with the required solvent. The resulting solution was filtered to remove any insoluble species, if necessary, and transferred into an NMR J. Young tube. A sealed D_2O capillary was added for locking and shimming if the solvent was TFE. An internal standard (5.0 μL, 0.247 M *tert*-butylbenzene in TFE or 0.964 M 1,4-difluorobenzene in TFE) was placed in the NMR J. Young tube as well. A nucleophile was added to the NMR J. Young tube by a micropipet, and the tube was pressurized with Ar. ^{1}H NMR spectroscopy was used to monitor the reaction progress. After a reaction was finished, a syringe with a long needle was used to measure the volume of the reaction solution.

Entries 1−3 (Table 1). **6**/**7**/**8** (10/12/10 mg, 18/18/18 μmol) and 0.042 mL of HBF_4 (49% w/w with water, 0.30 mmol of HBF_4, 1.5 mmol of H_2O) were combined with 0.60 mL of TFE. The solutions of **6** and **7** were filtered and the concentrations of the target complexes determined using ^{1}H NMR integration upon addition of *tert*-butylbenzene as an internal standard.

Entry 4 (Table 1). **7** (8.8 mg, 13 μmol) and 0.0204 mL (0.25 mmol) of TFA were combined with 0.60 mL of TFE. The solution was filtered, and the concentrations of the target complexes were determined using ^{1}H NMR integration upon addition of *tert*-butylbenzene as an internal standard.

Entry 5 (Table 1). **7** (13 mg, 20 μmol) and 0.0532 g (0.40 mmol) of $NaOOCCF_3$ were added to 0.60 mL of TFE. The solution was filtered, and the concentrations of the target complexes were determined using ^{1}H NMR integration upon addition of *tert*-butylbenzene as an internal standard.

Entry 6 (Table 1). **7** (6.0 mg, 9.1 μmol) was combined with 0.40 mL of AcOH-d_4 and 0.20 mL of D_2O. The mixture was filtered and combined with 0.0247 g (0.18 mmol) of $NaOOCCF_3$ in an NMR J. Young tube. The solution was filtered, and the concentrations of the target complexes were determined using ^{1}H NMR integration upon addition of *tert*-butylbenzene as an internal standard.

Entries 7−9 (Table 1). **6**/**7**/**8** (10/8.5/8.0 mg, 18/13/13 μmol) was dissolved in 0.60 mL of DMSO-d_6 and combined with 0.0274/0.0196/0.0193 mL (0.34/0.28/0.24 mmol) of TFA.

Entry 10 (Table 1). **7** (12 mg, 18 μmol) was dissolved in 0.60 mL of DMSO-d_6.

Entry 11 (Table 1). **7** (10.4 mg, 19.4 μmol) was dissolved in 0.60 mL of DMSO-d_6 and combined with 0.0296 mL (0.387 mmol) of TFA and 50 μL (2.8 mmol) of water.

Entry 12 (Table 1). **7** (12 mg, 18.4 μmol) was dissolved in 0.60 mL of DMSO-d_6 and combined with 0.0502 g (0.369 mmol) of $NaOOCCF_3$.

Entries 13−15 (Table 1). **6**/**7**/**8** (3.0/2.0/5.0 mg, 2.7/2.6/7.9 μmol) was added to 0.60 mL of TFE-*d* and combined with 30/19/48 μL (0.24/0.15/0.38 mmol) of *N*,*N*-dimethylaniline. The solutions of **6** and **7** were filtered and the concentrations of the target complexes determined using ^{1}H NMR integration upon addition of *tert*-butylbenzene as an internal standard.

Entry 16 (Table 1). **7** (5.0 mg, 7.6 μmol) was dissolved in 0.60 mL of DMSO-d_6 and combined with 36 μL (0.29 mmol) of *N*,*N*-dimethylaniline.

General Procedure for Kinetics Studies. The reaction solution was prepared as indicated above (reactions of **6**−**8**, general procedure), and the reaction was performed in a temperature-equilibrated NMR probe. An internal standard (*tert*-butylbenzene) was placed in the NMR J. Young tube. A sealed D_2O capillary was used for locking and shimming purposes. The rate of disappearance of **7** was monitored. The experiment was repeated with different concentrations of *N*,*N*-dimethylaniline.

DFT Calculations. Theoretical calculations have been carried out with the Jaguar program package[17] using the density functional theory (DFT) method,[18] specifically the PBE-D3 functional, which was demonstrated to work well for kinetics and thermodynamics of a number of organometallic reactions,[19] and the LACVP relativistic basis set with two polarization functions. Full geometry optimization has been performed in the gas phase with the PBE functional, without constraints on symmetry. The optimized geometries then were used for single-point calculations of dispersion-corrected energy values using the PBE-D3 functional, as described previously.[19] The solvation Gibbs energies G(solv) in TFE were also found using single-point calculations utilizing a Poisson−Boltzmann continuum solvation model (PBF). For all species under investigation frequency analysis has been carried out. All energy minima have been checked for the absence of imaginary frequencies. All transition states possessed just one imaginary frequency. Using the intrinsic reaction coordinate method, reactants, products, and the corresponding transition states were proven to be connected by a single minimal energy reaction path. The dispersion-corrected total gas-phase Gibbs free energies (G(tot-D3)) at 298 K were produced in hartrees (1 hartree = 627.51

DOI: 10.1021/acs.organomet.9b00702
Organometallics 2020, 39, 142−152

kcal/mol). The standard reaction Gibbs energies in TFE, ΔG_{rxn}, in kcal/mol were calculated as follows:

$$\Delta G_{rxn} = 627.51 \times \left[\sum G(\text{tot-D3})_{products} - \sum_{gas\ phase} G(\text{tot-D3})_{reactants}\right] + \sum G(\text{solv})_{products} - \sum G(\text{solv})_{reactants} + \Delta nRT \ln(RT/P)$$

where Δn is the change in the number of moles in a balanced reaction equation on going from reactants to products. The standard state for all solutes is 1 M concentration.

■ ASSOCIATED CONTENT

Supporting Information

The Supporting Information is available free of charge at https://pubs.acs.org/doi/10.1021/acs.organomet.9b00702.

NMR spectra and computational details (PDF)

Cartesian coordinates of the calculated structures (XYZ)

■ AUTHOR INFORMATION

Corresponding Author

*E-mail for A.N.V.: avederni@umd.edu.

ORCID

Jiaheng Ruan: 0000-0003-0907-5685

Andrei N. Vedernikov: 0000-0002-7371-793X

Notes

The authors declare no competing financial interest.

■ ACKNOWLEDGMENTS

This work was supported by the National Science Foundation (CHE-1800089) and, in part, the US−Israel Binational Science Foundation (grant 2014254) and the Center for Catalytic Hydrocarbon Functionalization, an Energy Frontier Research Center Funded by the U.S. Department of Energy, Office of Science, Office of Basic Energy Sciences, under Award Number DE-SC0001298.

■ REFERENCES

(1) (a) Shilov, A. E.; Shulpin, G. B. *Activation and Catalytic Reactions of Saturated Hydrocarbons in the Presence of Metal Complexes*; Kluwer: Boston, 2000. (b) Campbell, A. N.; Stahl, S. S. Overcoming the "Oxidant Problem": Strategies to Use O_2 as the Oxidant in Organometallic C-H Oxidation Reactions Catalyzed by Pd (and Cu). *Acc. Chem. Res.* **2012**, *45*, 851−863. (c) Boisvert, L.; Goldberg, K. I. Reactions of Late Transition Metal Complexes with Molecular Oxygen. *Acc. Chem. Res.* **2012**, *45*, 899−910. (d) He, J.; Wasa, M.; Chan, K. S. L.; Shao, Q.; Yu, J.-Q. Palladium-Catalyzed Transformations of Alkyl C-H Bonds. *Chem. Rev.* **2017**, *117*, 8754−8786. (e) Gunsalus, N. J.; Koppaka, A.; Park, S. H.; Bischof, S. M.; Hashiguchi, B. G.; Periana, R. A. Homogeneous Functionalization of Methane. *Chem. Rev.* **2017**, *117*, 8521−8573.

(2) (a) Geletii, Y. V.; Shilov, A. E. Catalytic Oxidation of Alkanes by Molecular Oxygen - Oxidation of Methane in the Presence of Platinum Salts and Heteropoly Acids. *Kinetics and Catalysis* **1983**, *24*, 413−416. (b) Lin, M. R.; Shen, C. Y.; Garcia-Zayas, E. A.; Sen, A. Catalytic Shilov Chemistry: Platinum Chloride-catalyzed Oxidation of Terminal Methyl Groups by Dioxygen. *J. Am. Chem. Soc.* **2001**, *123*, 1000−1001. (c) Bar-Nahum, I.; Khenkin, A. M.; Neumann, R. Mild, Aqueous, Aerobic, Catalytic Oxidation of Methane to Methanol and Acetaldehyde Catalyzed by a Supported Bipyrimidinylplatinum−Polyoxometalate Hybrid Compound. *J. Am. Chem. Soc.* **2004**, *126*, 10236−10237.

(3) Watts, D.; Wang, D.; Zavalij, P. Y.; Vedernikov, A. N. Novel Sulfonated CNN Pincer Ligands for Facile C−H Activation at a Pt(II) Center. *Isr. J. Chem.* **2017**, *57* (10−11), 1010−1022.

(4) Watts, D.; Wang, D.; Adelberg, M.; Zavalij, P. Y.; Vedernikov, A. N. C−H and O_2 Activation at a Pt(II) Center Enabled by a Novel Sulfonated CNN Pincer Ligand. *Organometallics* **2017**, *36* (1), 207−219.

(5) Watts, D.; Zavalij, P. Y.; Vedernikov, A. N. Consecutive C−H and O_2 Activation at a Pt(II) Center To Produce Pt(IV) Aryls. *Organometallics* **2018**, *37* (22), 4177−4180.

(6) Labinger, J. A.; Bercaw, J. E. Understanding and Exploiting C-H Bond Activation. *Nature* **2002**, *417*, 507−514.

(7) Khusnutdinova, J. R.; Zavalij, P. Y.; Vedernikov, A. N. C−O Coupling of LPt ^{IV} Me(OH)X Complexes in Water (X = ^{18}OH, OH, OMe; L = Di(2-Pyridyl)Methane Sulfonate). *Organometallics* **2007**, *26* (14), 3466−3483.

(8) Vedernikov, A. N.; Binfield, S. A.; Zavalij, P. Y.; Khusnutdinova, J. R. Stoichiometric Aerobic Pt ^{II} − Me Bond Cleavage in Aqueous Solutions to Produce Methanol and a Pt ^{II} (OH) Complex. *J. Am. Chem. Soc.* **2006**, *128* (1), 82−83.

(9) (a) Luinstra, G. A.; Labinger, J. A.; Bercaw, J. E. Mechanism and Stereochemistry for Nucleophilic Attack at Carbon of Platinum(IV) Alkyls: Model Reactions for Hydrocarbon Oxidation with Aqueous Platinum Chlorides. *J. Am. Chem. Soc.* **1993**, *115* (7), 3004−3005. (b) Canty, A. J.; Jin, H.; Skelton, B. W.; White, A. H. Oxidation of complexes by $(O_2CPh)_2$ and $(ER)_2$ (E = S, Se), including structures of [cyclic] $Pd(CH_2CH_2CH_2CH_2)(SePh)_2(bpy)$ (bpy = 2,2′-bipyridine) and $MMe_2(SePh)_2(L_2)$ (M = Pd, Pt; L_2 = bpy, 1,10-phenanthroline) and C···O and C···E bond formation at palladium(IV). *Inorg. Chem.* **1998**, *37* (16), 3975−3981. (c) Williams, B. S.; Goldberg, K. I. Studies of Reductive Elimination Reactions To Form Carbon-Oxygen Bonds from Pt(IV) Complexes. *J. Am. Chem. Soc.* **2001**, *123* (11), 2576−2587. (d) Smythe, N. A.; Grice, K. A.; Williams, B. S.; Goldberg, K. I. Reductive Elimination and Dissociative β-Hydride Abstraction from Pt(IV) Hydroxide and Methoxide Complexes. *Organometallics* **2009**, *28* (1), 277−288. (e) Pawlikowski, A. V.; Getty, A. D.; Goldberg, K. I. Alkyl Carbon-Nitrogen Reductive Elimination from Platinum(IV)-Sulfonamide Complexes. *J. Am. Chem. Soc.* **2007**, *129* (34), 10382−10393.

(10) Vedernikov, A. N.; Fettinger, J. C.; Mohr, F. Synthesis and Reactivity of Dimethyl Platinum(IV) Hydrides in Water. *J. Am. Chem. Soc.* **2004**, *126* (36), 11160−11161.

(11) Aseman, M. D.; Nabavizadeh, S. M.; Niroomand Hosseini, F.; Wu, G.; Abu-Omar, M. M. Carbon−Oxygen Bond Forming Reductive Elimination from Cycloplatinated(IV) Complexes. *Organometallics* **2018**, *37* (1), 87−98.

(12) Lersch, M.; Tilset, M. Mechanistic Aspects of C−H Activation by Pt Complexes. *Chem. Rev.* **2005**, *105* (6), 2471−2526.

(13) Adams, D. J.; Johns, B.; Vedernikov, A. N. Methyl Transfer Reactivity of Pentachloromethylplatinate(IV) Anion with a Series of N-Nucleophiles. *J. Organomet. Chem.* **2019**, *880*, 22−28.

(14) Stevens, T. E.; Smoll, K. A.; Goldberg, K. I. Direct Formation of Carbon(sp^3)−Heteroatom Bonds from Rh^{III} To Produce Methyl Iodide, Thioethers, and Alkylamines. *J. Am. Chem. Soc.* **2017**, *139* (23), 7725−7728.

(15) Mironov, O. A.; Bischof, S. M.; Konnick, M. M.; Hashiguchi, B. G.; Ziatdinov, V. R.; Goddard, W. A.; Ahlquist, M.; Periana, R. A. Using Reduced Catalysts for Oxidation Reactions: Mechanistic Studies of the "Periana-Catalytica" System for CH_4 Oxidation. *J. Am. Chem. Soc.* **2013**, *135* (39), 14644−14658.

(16) Otto, S.; Roodt, A. Reactivity Studies of Trans-[PtClMe$(SMe_2)_2$] towards Anionic and Neutral Ligand Substitution Processes. *J. Organomet. Chem.* **2006**, *691* (22), 4626−4632.

(17) *Jaguar, version 8.4*; Schrödinger, LLC: New York, NY, 2014.

(18) Parr, R. G.; Yang, W. *Density-functional Theory of Atoms and Molecules*; Oxford University Press: Oxford, 1989.

(19) Hopmann, K. H. How Accurate is DFT for Iridium-Mediated Chemistry? *Organometallics* **2016**, *35*, 3795−3807.

DOI: 10.1021/acs.organomet.9b00702
Organometallics 2020, 39, 142−152